

The role of the Josephson-Anderson equation in superfluid helium*

Richard E. Packard

Physics Department, University of California, Berkeley, California 94720

This article explains how a simple equation describing the time evolution of a superfluid's quantum phase can be used as a powerful tool to rapidly deduce exact magnitudes of physical observables in situations involving very complex vortex motion. The equation has been used to simplify the understanding of new phenomena, such as vortex precession. Applications of the equation have also led to solutions of long-standing problems, such as the nucleation of vortices, and to new technology, such as the superfluid gyroscope. The article begins by presenting some basic ideas of superfluidity. This discussion leads to the concept of the quantum phase of the superfluid state and to the prediction that vorticity is quantized. Next a discussion is presented of the phase evolution equation, introduced by Josephson and developed further by Anderson. The utility of the equation is demonstrated by making certain general predictions about the consequences of vortex motion. Two experiments, one in ^3He and another in ^4He , are then described in the context of the phase evolution equation. In the first, the precession frequency of a single vortex filament is easily explained in the context of the equation. In the second, quantized dissipation processes are observed which give detailed information about the creation of quantized vortices. The article concludes by showing how these latter experiments have led to the development of a superfluid sensor of absolute rotation. Although the article focuses on results emerging from the author's own laboratory, the footnotes lead the reader to some of the parallel ongoing projects, especially in the case of the ^4He research at Orsay/Saclay in France, the University of Minnesota, and the University of Trento, Italy. [S0034-6861(98)00702-8]

CONTENTS

I. Introduction	641
II. Vortex Precession: Demonstration of the Josephson Frequency	644
III. Discrete Phase Slippage	647
IV. Summary and Recent Developments	650
Acknowledgments	651
References	651

I. INTRODUCTION

Superfluidity in ^4He was discovered in the late 1930s (Kapitza, 1938, Allen and Misener, 1939) when it was observed that liquid ^4He , cooled below 2.17 K, could flow through exceedingly small passages without appreciable driving pressures. These discoveries were followed quickly by the theories of Tisza (1938) and Landau (1941), which quantified a two-fluid picture of the superfluid state. The description modeled the system as two interpenetrating fluids. The superfluid component is characterized by zero entropy, zero viscosity, and strictly potential flow. The normal component, consisting of the elementary excitations of the system (phonons and rotons), carries entropy and possesses viscosity. Landau introduced a complete set of hydrodynamic equations which blend together Euler and Navier-Stokes representations of the two components.

In a parallel development, Fritz London realized that the concept of dissipation-free flow was similar to the

“motion” of atomic electrons. He conjectured that superfluidity might be a manifestation of quantum mechanics on a macroscopic scale (London, 1954). Superfluid ^4He would be a quantum liquid.

A few years after the close of World War II another important advance was made when Onsager (1949) attempted to find the form of a macroscopic quantum wave function appropriate for superfluids.¹ He reached two related conclusions: (1) Superfluid circulation κ must be quantized in integral multiples of Planck's constant divided by the mass of the helium atom: $\kappa_0 = h/m_4$. (2) Vorticity could exist in a superfluid in the form of vortex lines with quantized circulation. These ideas were independently discovered by Feynman (1955). Their reasoning proceeds as follows.

The general form of the superfluid fraction's wave function is

$$\psi = |\psi| e^{i\phi(r)}. \quad (1)$$

Here the squared magnitude, $|\psi|^2$, can be thought of as being proportional to the superfluid density ρ_s . If the wave function is inserted into the standard quantum-mechanical expression for current, and variations in the wave-function magnitude are negligible, one obtains the result

¹It can be rigorously shown from microscopic many-particle physics that simple superfluid systems can be described by a function possessing amplitude and phase. That function satisfies a single-particle Schrödinger-like equation and the number current can be computed by applying the usual single-particle current operator to the function. The terms macroscopic wave function and order parameter are used to describe the same entity.

*This article is based on a colloquium that the author delivered at several universities in 1996.

$$\vec{J}_s = |\psi|^2 \frac{\hbar}{m} \vec{\nabla} \phi. \quad (2)$$

By analogy with ordinary fluid flow, if ρ_s is associated with the square of the wave function's amplitude, then the superfluid velocity v_s is equal to the phase gradient term:

$$\vec{v}_s = \frac{\hbar}{m} \vec{\nabla} \phi. \quad (3)$$

Thus the quantum-mechanical phase appears as a scaled velocity potential. Since the wave function must be single valued, we are led directly to the condition for quantization of circulation,

$$\kappa \equiv \oint \vec{v}_s \cdot d\vec{l} = \frac{\hbar}{m} \oint \vec{\nabla} \phi \cdot d\vec{l} = n \frac{h}{m},$$

$$n = 0, \pm 1, \pm 2, \pm 3, \dots \quad (4)$$

The circulation is quantized in units of $\kappa_0 = h/m$. The mass here is the bare atomic mass of the entity, which is the "fundamental superfluid particle" (Morrison and Lindesay, 1977). For ${}^4\text{He}$, $m = m_4$. Superfluidity also exists in two different phases in the isotope ${}^3\text{He}$, below 2×10^{-3} K. These states are believed to be superfluids of Cooper-paired particles. Of the two phases, designated ${}^3\text{He-A}$ and ${}^3\text{He-B}$, the latter has a macroscopic wave function similar to that of ${}^4\text{He}$ and it is therefore expected that, when referring to ${}^3\text{He-B}$, the mass in Eq. (4) and in the expression for κ_0 would be $2m_3$.

It is possible for vorticity to exist in a superfluid in the form of vortex lines with quantized circulation. The presence of quantized vortex lines in rotating superfluid ${}^4\text{He}$ was first detected by Hall and Vinen (1956). A few years later, Rayfield and Reif (1964) discovered superfluid quantized vortex rings in ${}^4\text{He}$. Subsequently, hundreds of papers have been written about quantized vortices in both ${}^4\text{He}$ and ${}^3\text{He}$, revealing many facets of these superfluid line defects.² Included in this vast body of research are experiments, performed at Berkeley, which photograph the vortex positions in ${}^4\text{He}$ (Yarmchuk *et al.*, 1979).

A vortex consists of fluid flowing in concentric rings around a central core, with a velocity that diminishes inversely with distance from the vortex center. Superfluidity breaks down within the core, which is of atomic dimension. Planes of constant phase, ϕ , radiate from the vortex core. The phase advances by precisely 2π as the vortex is encircled.

In this article, we shall focus on phenomena related to the passage of vortex lines between two separated reference points. Figure 1 shows the lines of constant phase as a vortex line, perpendicular to the page, moves between two points lying on opposite sides of a flow passage bounded by plane parallel sides. It is apparent in

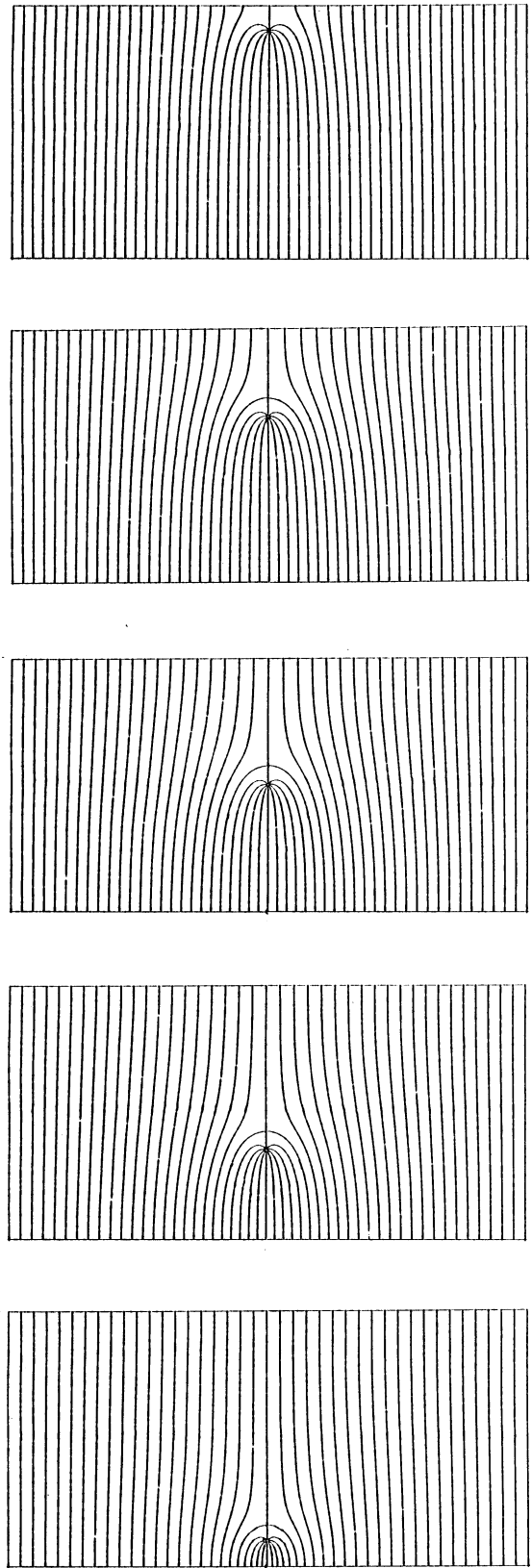


FIG. 1. A plot of lines of constant phase during the passage of a quantized vortex line across a tube. The velocity through the tube is proportional to the phase gradient. After the passage of the vortex there are ten fewer lines of constant phase. Since each line represents a phase difference of $\pi/5$, the ten missing lines represent a 2π change.

²A review of quantized vortices in ${}^4\text{He}$ is presented in Donnelly (1991). A review of vortices in ${}^3\text{He}$ is presented in Krusius (1993).

the figure that, as the vortex moves from the top to the bottom, the phase difference between two points at opposite ends of the passage changes by 2π . Such a vortex passage is referred to as a “ 2π phase slip,” a term that is most descriptive if the vortex passage takes place on a time scale that is short compared to some observation time.

The equation that is the focus of this article can be derived by several means. We shall outline here the argument of Anderson, which was described in more detail in this same journal over thirty years ago (Anderson, 1966). The argument is made in the context of a second-quantization description of condensed matter. Anderson shows that the number operator \hat{N} is canonically conjugate to the phase operator $\hat{\phi}$ which projects the phase of the many-particle wave function. His proof involves constructing a wave packet for the eigenfunctions of \hat{N} in terms of the eigenfunctions of $\hat{\phi}$.

Canonically conjugate variables, like position and momentum, have corresponding operators whose commutator is purely imaginary. The commutation relation for \hat{N} and $\hat{\phi}$ is

$$[\hat{N}, \hat{\phi}] = i. \quad (5)$$

For such canonically conjugate operators the equations of motion of their expectation values are given by Hamilton's equations. Thus

$$\hbar \frac{\partial \langle \hat{N} \rangle}{\partial t} = \left\langle \frac{\partial \hat{H}}{\partial \phi} \right\rangle, \quad (6)$$

$$\hbar \frac{\partial \langle \hat{\phi} \rangle}{\partial t} = - \left\langle \frac{\partial \hat{H}}{\partial N} \right\rangle = -\mu, \quad (7)$$

where the chemical potential μ is defined as the increase in internal energy when a single particle is added to the system, keeping entropy and volume constant.

We consider two points in the fluid of density ρ , with average phase ϕ_1 and ϕ_2 . If at these points the corresponding chemical potential is μ_1 and μ_2 , then Eq. (7) becomes

$$\begin{aligned} \frac{\partial(\phi_2 - \phi_1)}{\partial t} &= - \frac{(\mu_2 - \mu_1)}{\hbar} \\ &= - \frac{m[(P_2 - P_1)/\rho + (v_s^2/2)_2 - (v_s^2/2)_1]}{\hbar}. \end{aligned} \quad (8)$$

In the last step we include the average kinetic energy of the particles in the definition of the chemical potential. For simplicity, we are focusing on situations in which the temperature is constant, so that the chemical potential difference is determined only by the pressure difference and the kinetic-energy difference. The mass entering the equation is the bare mass of the objects in the quantum state: either the ^4He atom or a ^3He Cooper pair.

Equation (8) is the focus of this article. It is the equation of motion of the quantum phase difference between two points in a superfluid. Because this equation was

first written in the context of superconductivity by Josephson (1962), it is often called the Josephson phase evolution equation. Since Anderson derived the result in the broader context of a more general quantum liquid, we shall refer to it here as the Josephson-Anderson equation or simply the JA equation. If both sides of Eq. (8) are differentiated with respect to position, and if Eq. (3) is used to substitute the velocity for the phase gradient, then Eq. (8) becomes Euler's equation for a vorticity-free, perfect fluid, $\dot{\vec{v}}_s = -\vec{\nabla}P/\rho - \vec{\nabla}(v_s^2/2)$, except for the important distinction that the total mass density ρ appears in place of the superfluid mass density ρ_s . Landau derived this equation of motion for the superfluid component long before the importance of the quantum phase was appreciated.

Since in Eq. (8) the time derivative of the phase difference is [from Eq. (3)] equivalent to the time derivative of velocity, and the chemical potential difference is equivalent to a force, it would seem that this equation is only equivalent to Newton's second law. It seems to describe the accelerated flow of a perfect fluid. However, the real utility arises because quantized vortices exist in superfluids, and the motion of the vortices commonly enters many interesting dynamic situations.

In this article we shall be interested in situations where single quantized vortex lines pass periodically at some frequency f between two points. For simplicity we first consider two separated points where the flow velocity is essentially zero. Since the phase change per vortex passage is 2π , the rate of change of phase is $2\pi f$. For a given pressure difference this frequency can be calculated from Eq. (8). Solving for the Josephson-Anderson frequency f_{JA} , one gets

$$f_{JA} = - \frac{(\mu_2 - \mu_1)}{h} = - \frac{m}{\rho h} (P_2 - P_1). \quad (9)$$

The constants entering Eq. (9) imply that a 1-Pa pressure head will cause 69×10^3 phase slips per second for ^4He and 184×10^3 per second for Cooper-paired ^3He . Note that the JA frequency is independent of the path over which the vortices move as the tube is crossed, however complex that motion might be. All the complexity of the vortex dynamics is removed from the frequency determination because the phase can change by only 2π .

Another simple calculation leads to the energy change in organized flow due to the passage of a single vortex across a flow tube, e.g., Fig. 1. Such a process may occur when a vortex is created by stochastic processes (e.g., thermal or quantum) near a wall, at a characteristic critical current I_c . Multiplying both sides of Eq. (8) by the mass current I_c and integrating gives

$$I_c \int d(\phi_2 - \phi_1) = \frac{-m}{\hbar} \int \frac{I_c \delta P}{\rho} dt. \quad (10)$$

The integrand on the right is the instantaneous power extracted from the flow. The integration over a 2π phase change gives, on the right-hand side, the energy removed from the flow by a 2π phase slip. The left-hand side is just $2\pi I_c$. Thus

$$\delta E \approx -\frac{hI_c}{m} = -\kappa_o I_c. \quad (11)$$

We have assumed here that the current change due to the phase slip is small compared to the critical current, an approximation that is not always true, especially near the transition temperature. Like Eq. (9) for f_{JA} , Eq. (11) for the energy decrease is independent of the vortex's path and is therefore a beautiful simplification of a complicated process. The energy-loss mechanism of phase slippage is the fundamental process by which an inviscid superfluid can lose energy. The kinetic energy carried away by the vortex is presumably transformed to heat when the vortex annihilates by collision with a wall.

If the flow tube has an effective length l_{eff} , Eq. (3) gives the velocity decrement corresponding to the 2π slip as

$$\delta v_s = \frac{h}{ml_{\text{eff}}} = \frac{\kappa_o}{l_{\text{eff}}}. \quad (12)$$

When quantized vortices are created in large flow tubes, they dissipate energy continuously in a process known as a vortex mill (Schwarz, 1990). By contrast, discrete 2π phase slips are found (see below) to occur in small apertures. We are concerned here with small flow apertures whose effective lengths are on the order of 10^{-6} m. For this situation, the velocity decrement, Eq. (12), is about 0.1 m/s for a 2π slip, and the energy decrement³ is of the order of 10^{-17} J.

The remainder of this article describes two experiments that are easily interpreted in the context of the phase evolution equation. The first relies on the Josephson frequency relation, Eq. (9), and the second involves Eqs. (11) and (12) for δE and δv_s .

II. VORTEX PRECESSION: DEMONSTRATION OF THE JOSEPHSON FREQUENCY

For the first experiment, a digression is required because the observation of the Josephson frequency was a serendipitous spinoff of another experiment. We begin by briefly describing an experiment in superfluid ^3He -B designed to determine whether circulation is quantized in that system (Davis *et al.*, 1990). The goal is to answer two questions: (1) Is circulation quantized in ^3He ? (2) Does the quantum of circulation involve twice the atomic mass of ^3He ? The latter is a necessary consequence of the Cooper-pairing idea, which is invoked to explain how a Fermi system can display superfluidity.

The experimental technique follows that of Vinen (1961), invented to determine the circulation in superfluid ^4He . One determines the plane of vibration of a thin stretched wire surrounded by superfluid. If the cross section of the wire is round, the vibration plane is stationary in the absence of circulation. If there is fluid

³The vortex carries away the energy from the tube flow. It is not clear, however, how the vortex eventually transfers this energy to heat.

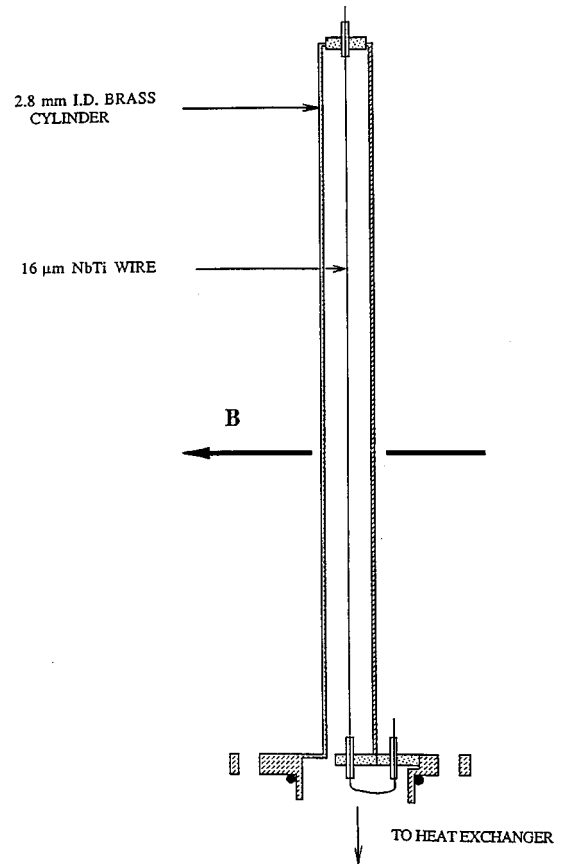


FIG. 2. A sketch of the vibrating wire apparatus to measure superfluid circulation. A fluid circulation around the wire causes a precession of the plane of vibration.

circulation κ around the vibrating wire, then a sidewise force exists. This effect is a result of Bernoulli's principle, the flow velocity is faster on one side of the wire than on the other, and is often called the Magnus force. The sidewise force causes the vibration plane to precess at frequency f_c proportional to the circulation. Specifically,

$$\kappa = \frac{2\pi\lambda f_c}{\rho_s} \quad (13)$$

where λ is the wire's lineal mass density.

Since the vibrating wire technique was successful in demonstrating quantized circulation in ^4He , it seemed desirable to use the same idea in ^3He . The main technical problem with applying the technique to ^3He is that at temperatures above $T/T_c = 0.2$ the normal-component viscosity is so great that the wire's vibration is damped to zero in a time less than the expected precession period. However, in the mid-1980s, cryogenic techniques finally achieved the temperature range of interest (Guénault *et al.*, 1986). We then constructed a rotating refrigerator that could cool superfluid to 165 μK (Close *et al.*, 1990). At these temperatures, our vibrating wire exhibits a decay time of several seconds, which is adequate for the circulation measurements.

Figure 2 shows a sketch of the vibrating wire apparatus. The 16- μm -diameter wire surrounded by superfluid

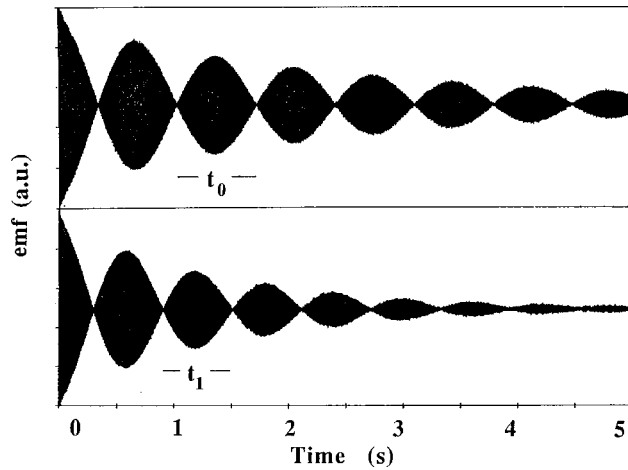


FIG. 3. The voltage induced across the ends of the vibrating wire, showing the envelope of the fundamental resonance frequency. The beat pattern is due both to circulation around the wire and to the asymmetry of the wire cross section. Top trace: voltage in the absence of rotation. Bottom trace: voltage in the presence of rotation. The precession frequency is higher in the bottom trace. The difference in decay time of the two traces is due to a small temperature difference between the two trials.

^3He exhibits a fundamental resonance at 347 Hz. A magnetic field of 50 mT is applied perpendicular to the wire. The wire is “plucked” by the magnetic force due to a current pulse passed through the wire. During the subsequent free-ringing decay, the voltage across the wire is monitored. If the vibration plane is perpendicular to the magnetic field, there is a maximum emf induced along the wire. If the plane is parallel with the field, there is no emf induced. The precession of the plane of vibration should therefore produce a beat signal across the ends of the wire.

Figure 3 shows some typical signals. The upper trace is taken when the cryostat is not rotating and presumably is the characteristic signal in the absence of fluid circulation around the wire. The fact that there is any precession at all is a consequence of the wire’s not having a round cross section. The lower trace is the characteristic signal when the cryostat is rotating. It is clear that there is a difference in the precession rates of the vibration plane. From the difference in the precession rates, one can use a modified form (Whitmore and Zimmermann, 1968) of Eq. (13) to compute the fluid circulation. The experiment consists of rotating the refrigerator at increasing angular velocities and continuously measuring the precession rate of the wire. The rotation will cause circulation to form around the wire.

Figure 4 shows the observed circulation in units of $h/2m_3$. The quantization of the values is clear, and the quantum unit is seen to have the double Cooper-pair mass as expected. This result confirms the idea that $^3\text{He-B}$ is a phase-coherent quantum fluid and that Cooper pairing characterizes this state of matter.

The description of this experiment so far is a preamble to the discussion of the utility of the JA phase evolution equation. The phenomena relevant to this ar-

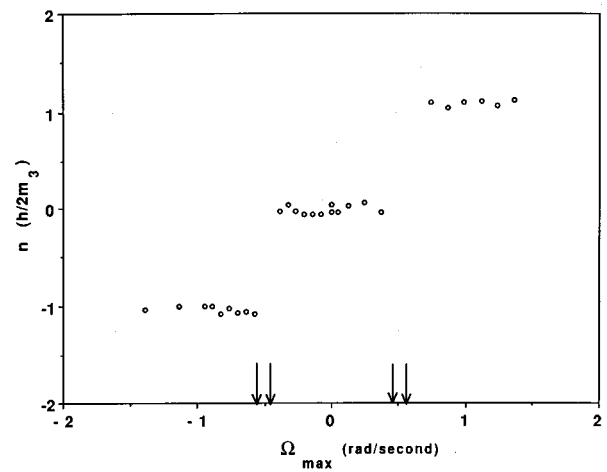


FIG. 4. The circulation around the wire as a function of the highest rotation speed of the cryostat. The vertical axis is in units of $h/2m_3$ and contains no adjustable constants. The circulation was unstable for the values of angular velocity between the two sets of arrows.

ticle arise from the observation of the signal when circulation is trapped metastably on the wire. This trapping results when the cryostat is first rotated at speeds that stabilize a single quantum of circulation. A subsequent slow deceleration of the cryostat to rest usually leaves the circulation metastably trapped on the wire. In effect there is a singly quantized vortex whose core is the solid wire. The vortex terminates at the top and bottom of the cylinder. Since there is zero dissipation in the superfluid, the vortex flow can persist indefinitely.

On some occasions the trapped vorticity decays as shown in Fig. 5. Presumably after several hours some mechanical disturbance has broken one end of the vortex free from the walls and let it become terminated on the inside wall of the metal cylinder surrounding the vibrating wire. The vortex then “unzips” itself from the wire so that the system can approach the circulation-free

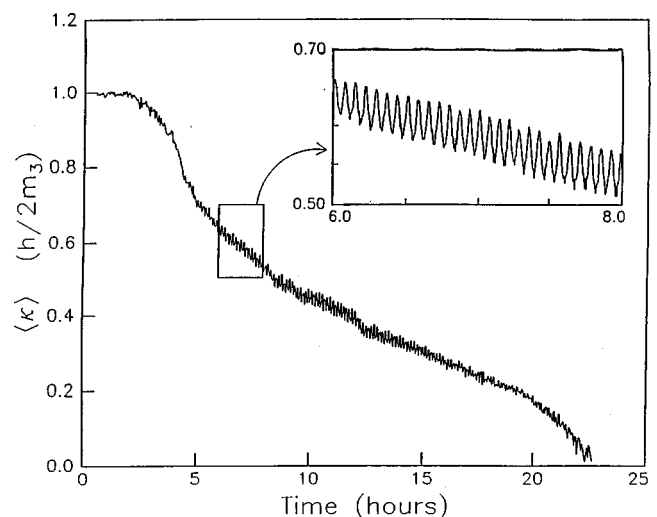


FIG. 5. The decay of circulation as a function of time. The figure inset shows the oscillations due to vortex precession.

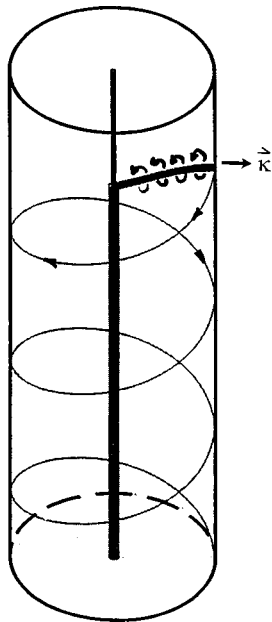


FIG. 6. A model of the vortex “unzipping” from the wire.

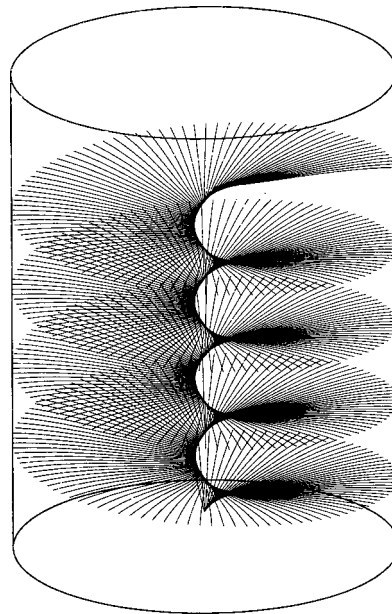


FIG. 7. A numerical simulation of the vortex motion by K. W. Schwarz (1993a).

ground state. Since the precession rate of the vibration plane is determined by the average circulation along the wire, a quantized vortex, partially attached to the wire, results in a nonquantized apparent circulation.

The feature of interest here is the small oscillation in the average circulation which accompanies the decay. The inset to Fig. 5 displays the oscillation more clearly. The question, of course, is, what is the physical mechanism underlying this oscillation? Our model of the physical process involved is shown in Fig. 6. Here we assume that a quantized vortex is partially detached from the wire and passes between the wire and the outer cylinder. The detached filament may rotate around the central wire, reminiscent of a one-bladed helicopter. The existence of the observable signal, correlated with the precession, is a consequence of the vibrating wire's being located slightly off axis. In order to conserve energy, as the vortex filament precesses around the off-axis wire, the attachment point on the wire must oscillate along the wire at the same frequency as the precession. This will lead to an oscillation signal like that seen in the figure (Zieve *et al.*, 1992; Zieve, 1992).

There are several approaches that show that such motion will lead to the observed frequency. Perhaps the most direct and complete approach is to perform a numerical integration of the vortex equations of motion. By making use of a sophisticated algorithm and substantial computing power, Schwarz (1993a) and Sonin (1994) obtained the helical path shown in Fig. 7. The numerical simulation confirms the model of the vortex precession and shows the delicate details of the motion. The rotation frequency, which can be deduced from the shape of the vortex line, agrees closely with that found in the experiment (Zieve *et al.*, 1992; Zieve, 1992). The agreement obtained here between the numerical simulation and the experiment is possibly the most stringent test of the numerical methods for vortex dynamics. Classical

vortices are not quantized, and the dynamics associated with the gradual dissipation of classical vorticity makes numerical simulation more difficult and comparison with experiments harder than the superfluid situation considered here.

The precession frequency can also be derived by assuming that the Magnus “lift” on the rotating vortex balances the tension in the still-trapped vortex section. In this kinematic approach we assume that the vortex helicopter model is correct and then proceed to balance forces (Zieve *et al.*, 1992; Zieve, 1992).

Still another approach is to use the idea that the rotation frequency must be the same as that of the smallest angular velocity of the container, which would favor the formation of the circulation along the wire. If the cylinder rotates faster, the vortex will go up the wire; if it rotates slower the point of attachment will move downward. Finding this critical angular velocity leads to the same formula as the force balance approach.

However, the approach relevant for our discussion is a direct consequence of the Josephson phase evolution equation (Misirpashaev and Volovik, 1992). As the end of the vortex filament precesses around the cylinder, the quantum phase difference between the ends of the cylinder changes by 2π for each revolution. The frequency of the precession is then just the Josephson-Anderson frequency and must be determined by the chemical potential difference across the two ends of the cylinder. This is computed in the following way:

Let n be the integer value of the vortex quantization on the lower part of the wire and $n - 1$ the quantization integer on the top section. The chemical potential μ is constant across each end of the cylinder but differs between the top and bottom. From our definition of chemical potential, the radial pressure dependence at the top end is given by

$$P_t(r) = \rho \left(\mu_t - \frac{v_s^2}{2} \right) = \rho \left(\mu_t - \frac{\kappa_o^2 (n-1)^2}{8\pi^2 r^2} \right). \quad (14)$$

On the bottom surface the pressure distribution is

$$P_b(r) = \rho \left(\mu_b - \frac{\kappa_o^2 n^2}{8\pi^2 r^2} \right). \quad (15)$$

The net force on the liquid is zero, so the force on the top and bottom of the container is equal and opposite. The force on each end is given by the area integral of the pressure over the ends. Computing this integral and equating the values on the top and bottom leads to the chemical potential difference ($\mu_b - \mu_a$) and subsequently to the Josephson-Anderson frequency of the filament's precession:

$$f_{JA} = \frac{\kappa_o(2n-1)}{4\pi^2(r_c^2 - r_w^2)} \ln \frac{r_w}{r_c}. \quad (16)$$

Here, r_c is the radius of the cylinder, r_w is the wire's radius, and κ_o is the circulation quantum. This formula describes the situation in which the vortex unzipping transforms the circulation around the wire from n quanta to $(n-1)$.

For the parameters of the ^3He experiment, $n=1$ and the formula predicts a Josephson frequency of 3.87×10^{-3} Hz. The measured value of the oscillation frequency is $3.90 \pm 0.05 \times 10^{-3}$ Hz. We also searched our data files collected during previous tests of the apparatus in ^4He . Here we discovered cases of oscillatory decay of circulation (Zieve *et al.*, 1993). In the case of ^4He , the circulation change was from $n=2$ to $n=1$. For this transition, using the circulation quantum for ^4He , the formula predicts a precession frequency of 17.4×10^{-3} Hz. The observed oscillations occurred at $17.2 \pm 0.3 \times 10^{-3}$ Hz.

It is interesting to point out that the chemical potential difference driving the precession is equivalent to a pressure head on the order of 2×10^{-7} Pa, comparable to that of a hydrostatic head of 0.2 nm of liquid ^3He . A state-of-the-art mechanical pressure gauge could not detect such a small difference. Yet this pressure difference is responsible for the entire observable effect of the vortex precession. The slow vortex precession frequency is a sensitive pressure gauge indeed.

As mentioned earlier, there are other approaches that will lead to Eq. (16). However, the phenomenon as interpreted in terms of the JA equation is particularly simple and elegant. The JA equation cannot tell us that the precession motion occurs but, given the observation that it does occur, the equation predicts the frequency of the phenomenon.

III. DISCRETE PHASE SLIPPAGE

As our second illustration of the utility of the JA equation, we focus on the concept of discrete phase slippage⁴ mentioned above and described by Eqs. (11)

⁴A recent review is given by Zimmermann (1996).

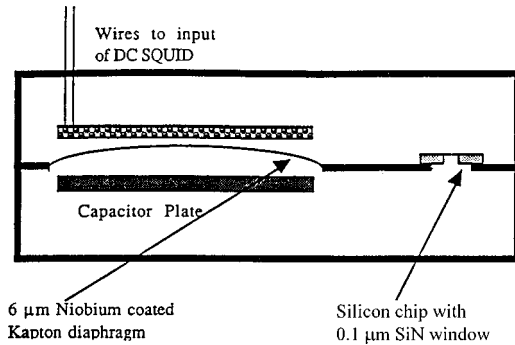


FIG. 8. Sketch of the generic superfluid oscillator used to observe discrete phase slips.

and (12). As shown by Eq. (11), the phase evolution equation leads to the prediction that if a single vortex crosses an aperture through which superfluid flows, a complete traversal of the aperture will remove $\kappa_o I_c$ of energy from the flow.⁵ I_c represents the critical current at which the vortex appears. It is believed that the vortices are nucleated near the walls as small half rings (Avenel *et al.*, 1993; Shiflett and Hess, 1995), which can enter the fluid by overcoming an energy barrier. As the current increases, the barrier falls, until thermal or quantum mechanisms permit vortex penetration into the bulk fluid. This initiates the phase slip process, which proceeds by some deterministic, but possibly complex, path (Schwarz, 1993b; Burkhart *et al.*, 1994).

A technique to detect these small dissipation events was developed by Avenel and Varoquaux (1987) about ten years ago. During the past decade their experiments have led the way to a new understanding of the phase slippage process in ^4He and the vortex nucleation phenomena which initiate the events. Figure 8 is a sketch of the generic apparatus used now in several laboratories. It is an oscillator that consists of two superfluid-filled regions, divided by a wall containing a flexible plastic partition and a submicron-sized aperture. In the experiments of Avenel and Varoquaux (1987) there is an additional low-flow-impedance path in parallel with the small aperture. In other laboratories, including Berkeley, there is often only the single microaperture as the path between the two volumes of superfluid. We fabricate our apertures in a 100-nm-thick silicon nitride "wall" using electron-beam lithographic techniques (Amar *et al.*, 1993). The oscillation frequency of the device, typically 2–60 Hz, is determined by the exchange between the potential energy stored in the displaced diaphragm and the kinetic energy stored in the flow through the aperture (Avenel and Varoquaux, 1987). Such a device is often referred to as a Helmholtz oscillator, but perhaps a more descriptive term would be diaphragm-aperture oscillator.

⁵This expression for the energy decrement describes the common situation in which the total flow energy is changed only slightly by the phase slip. If the flow energy is comparable to $\kappa_o I_c$, a more complex analysis is necessary.

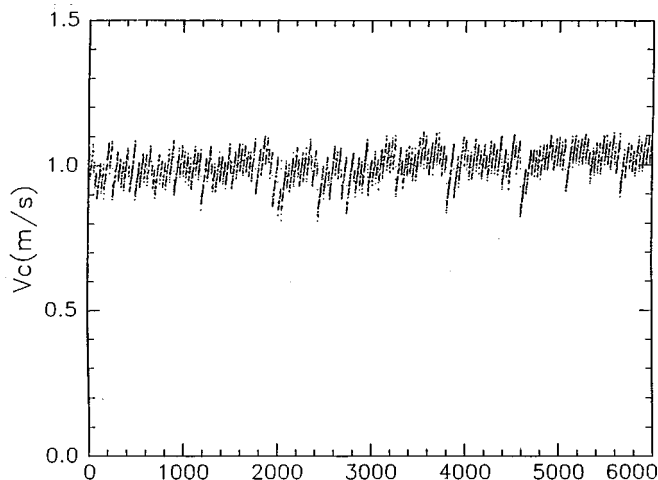


FIG. 9. The time evolution of a Helmholtz oscillator. Each point is the amplitude of one half cycle. The sudden drops in amplitude are the signature of the phase slips.

We coat the diaphragm on both sides with metal. A niobium film on one surface faces a nearby flat coil, which is the input coil of a SQUID-based displacement detector of the variety developed for gravity wave detection (Paik, 1976). This sensitive device can detect displacements of the diaphragm as small as 10^{-15} m/Hz^{1/2}. The other side of the diaphragm is typically coated with a normal metal (e.g., Au). An electric potential difference applied between this second surface and a nearby solid-metal electrode creates a force to move the diaphragm. There are various types of experiments that can be performed with this system. We focus here on experiments in which an oscillatory force, matched to the resonant frequency of the oscillator, is applied to the diaphragm.

Figure 9 shows the typical time evolution of the oscillation amplitude for a fixed amplitude of drive. Although the data shown here are from Berkeley (Amar *et al.*, 1992), very similar data in ⁴He are obtained at both Saclay (Avenel and Varoquaux, 1987) and Minnesota (Lindensmith *et al.*, 1996; Lindensmith, 1996). The figure displays the time dependence of the magnitude of every half cycle of oscillation. The amplitude can be seen to increase in time until a sudden event occurs which removes energy from the oscillator. The amplitude then climbs again until another event occurs. These sudden decrements in energy are caused when a microscopic quantized vortex is stochastically created in the aperture and subsequently moves across all the flow lines through the hole. Some of the flow energy in the oscillator is thereby transferred to the vortex flow and is ultimately lost when the vortex moves away, presumably annihilating at some distant wall.

Figure 10 is a distribution function showing the size of the abrupt drops in fluid velocity in the aperture (Amar *et al.*, 1992). Using the equations of motion of a quantized vortex in an inviscid fluid, it is possible to compute the energy transfer and velocity drop that should accompany the passage of a vortex across the hole (Huggins,

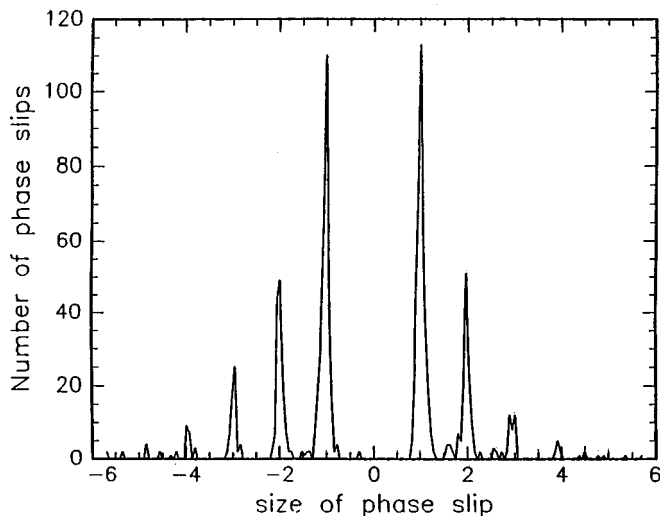


FIG. 10. A histogram of the size of the phase slips. The horizontal axis is drop in velocity amplitude in the aperture, δv . The units of the horizontal axis are κ_o/l_{eff} .

1970; Zimmermann, 1993). The calculations are complex and the result is not transparent at the outset. However, according to the JA phase evolution equation, the drop in energy due to a 2π phase slip is simply given by Eq. (11), $|\delta E| = \kappa_o I_c$. The ordinate in the figure is marked in units of κ_o/l_{eff} , which is the expected velocity decrement given in Eq. (12). The effective length here is determined from a measurement of the Helmholtz oscillator frequency and other experimental observables.

It is clear from the histogram that the flow velocity decrements are occurring in multiples of κ_o/l_{eff} . The first peak must correspond to a 2π phase slip. The higher peaks correspond to phase slips involving integral multiples of 2π . What is the origin of these higher multiples? One explanation is that n individual vortices are created in a cascade. We believe a more likely explanation is that a single vortex is nucleated and proceeds to evolve across the hole. During the evolution process, the vortex filament may become unstable and twist off, thus producing a vortex ring as well as the remainder of the filament. The further evolution of the free ring will itself produce a 2π phase change as it moves across all the flow lines. The remnant filament will complete its traversal of the aperture, giving another 2π . This process may then be responsible for the peak corresponding to a 4π slip. If n twistoff events occur, the total phase slip will be $(n+1)2\pi$.

There is supporting evidence for this interpretation of the existence of the peaks. We find that the peaks corresponding to higher-velocity decrements decrease in amplitude when the holes are made smaller. This may be because the smaller apertures permit vortex traversal before instabilities occur. Also, the peaks at higher values of velocity decrease as the temperature increases. This may be because at higher temperatures there is more normal fluid present to damp out instabilities in the vortex filament before they result in a twistoff event. When the entire oscillator is made very small (by con-

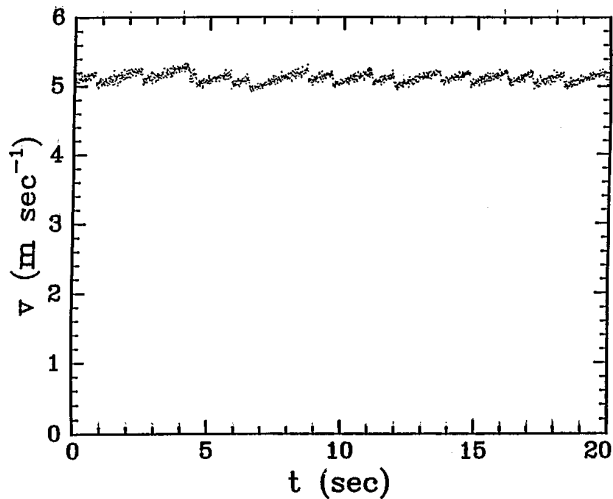


FIG. 11. The time evolution of amplitude of a miniature Helmholtz oscillation. The fluctuations in the critical oscillation amplitude are intrinsic and due to stochastic processes.

struction out of silicon using microfabrication techniques), the higher peaks disappear. We believe this is because the small oscillator⁶ is immune to acoustic disturbances that may induce instability in the vortex during its passage across the aperture. Figure 11 shows the time evolution of the oscillator amplitude for a very small oscillator constructed on a silicon wafer with microfabrication techniques. In this oscillator all the phase slips are of the 2π variety, and the critical velocity is insensitive to ambient vibration levels in the laboratory.

The apparent fluctuations in the critical oscillation amplitude are due to the intrinsic stochastic processes that mediate the vortex creation process. A statistical analysis (Varoquaux *et al.*, 1991) of these fluctuations in the critical velocity has led to a determination of an energy barrier that must be overcome to nucleate a microscopic vortex that initiates the phase slip. The data can be reasonably well explained by a model that supposes that the primordial vortex is in the form of a small half ring attached to the surface. If the half ring is to grow, the system must overcome an energy barrier whose height decreases as velocity along the surface increases. By assuming that the system obeys an Arrhenius law⁷ we can determine the velocity dependence of $E^* = E - k_B T \ln \Gamma$ where E is the velocity-dependent energy barrier, T is the temperature, and Γ is a dimensionless attempt frequency in units of 1 Hz. Studies of several different apertures (Steinhauer *et al.*, 1995a, 1995b; Lindensmith, 1996) reveal that there is a universal function for $E^*(v, T)$, which is displayed in Fig. 12. This function is reasonably well fit by the vortex half-ring model. Thus the study of phase slips, a phenomenon

⁶The internal volume of the oscillator is 0.43 mm^3 . For details see Steinhauer *et al.* (1995a, 1995b).

⁷The Arrhenius law states that a system in thermal equilibrium at temperature T can pass over an energy barrier of height E at the rate $\Gamma e^{-E/k_B T}$ where Γ is an attempt frequency.

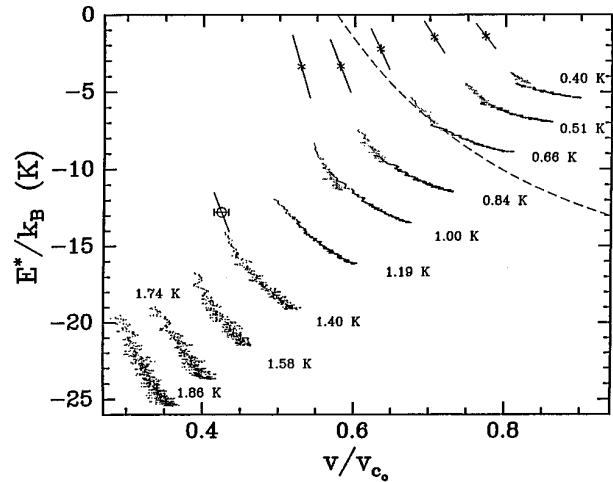


FIG. 12. The universal energy barrier E^* as a function of velocity and temperature. The asterisks and associated straight lines are taken from discrete phase slip experiments. The continuous curves with scatter are taken from DC flow experiments. The dashed line is a best fit to a half-ring vortex model. See Steinhauer *et al.* (1995a, 1995b) for a full description of the experiment.

suggested by Anderson as a model system for the JA equation, has led to a solution of the problem of the origin of vortices in superfluid ^4He !

Another spinoff of the phase slip research is a demonstration of a long held idea that superfluids can detect absolute rotation. The idea is best explained by reference to Fig. 13. The figure displays a superfluid-filled torus of radius R , which is interrupted by a septum containing a microaperture. We assume that the fluid is in the zero-circulation state and that the torus is slowly rotating at angular velocity Ω , about an axis perpendicular to the toroidal plane. The septum forces the bulk of the fluid to flow almost like a solid body, $v_s = \Omega R$, while

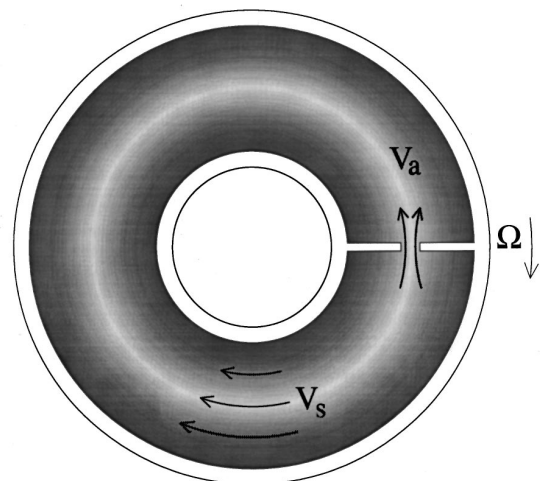


FIG. 13. A rotating torus showing the back flow induced in a small aperture. The velocity in the aperture is greater than the torus velocity, by the ratio of the torus circumference to the length of the aperture.

globally maintaining curl-free flow (Schwab, 1996). However, if $\oint \mathbf{v}_s \cdot d\mathbf{l} = 0$, integrated around the torus, the positive solid-body contribution from the bulk of the torus must be canceled by a negative contribution from the path within the aperture. Thus there must be a back flow in the aperture of magnitude v_a given by,

$$v_a = \Omega R \frac{2\pi R}{l_{\text{eff}}}. \quad (17)$$

The magnitude of the solid-body flow velocity is amplified by the ratio of the toroid circumference to the effective length of the microaperture. This ratio can reach 10^6 . So, if one can monitor the velocity in the aperture, one can detect a small absolute rotation. The phase slip critical velocity can serve as the “speedometer” for the aperture flow.

The realization of this idea is accomplished through the phase slippage phenomena described above. We connect a torus (like that shown in Fig. 13) in parallel with a flexible diaphragm, which is surrounded by the usual displacement detector and electrostatic driver (Schwab *et al.*, 1997). This system again is a diaphragm-aperture oscillator, but now the kinetic energy is contained in flow through the entire torus, dividing between a path through the aperture and a path through the rest of the torus. Again, one can detect single 2π phase slips and record the critical oscillation amplitude of the diaphragm. However, a rotation-induced flow in the aperture [Eq. (15)] will shift the apparent critical oscillation amplitude of the diaphragm. This shift is proportional⁸ to v_a .

Recently, two groups (Avenel and Varoquaux, 1997; Schwab *et al.*, 1997) demonstrated the principles described above to detect the motion of the Earth. At Berkeley, the toroidal device is built on a 1-cm-square silicon chip. The Earth’s rotation rate is measured by reorienting the plane of the torus with respect to the Earth’s rotation axis. This reorientation produces a shift in the apparent critical velocity for phase slippage. Figure 14 shows the critical oscillation amplitude of the diaphragm as a function of the orientation of the toroidal plane. The diaphragm amplitude, shown on the vertical axis, should vary as the cosine of the orientation angle. From the curve shown, we resolve the Earth’s rotation rate to $\approx 1\%$ in one hour. It should be possible to increase the device’s sensitivity by several orders of magnitude by adding multiple turns to the torus and increasing the scale of the macroscopic dimensions. As shown in Packard and Vitale (1992) and Avenel *et al.* (1994), the minimum detectable rotation rate is given by

$$\Omega_{\text{min}} = \frac{\pi r^2}{\sigma R} \frac{\Delta v_c}{\sqrt{f_o \tau}}. \quad (18)$$

Here r is the radius of the aperture, σ is the cross-section area of the torus, R is the torus’ radius, Δv_c is

⁸The superfluid gyroscope is analyzed by Packard and Vitale (1992). Similar ideas are described by Avenel *et al.* (1994).

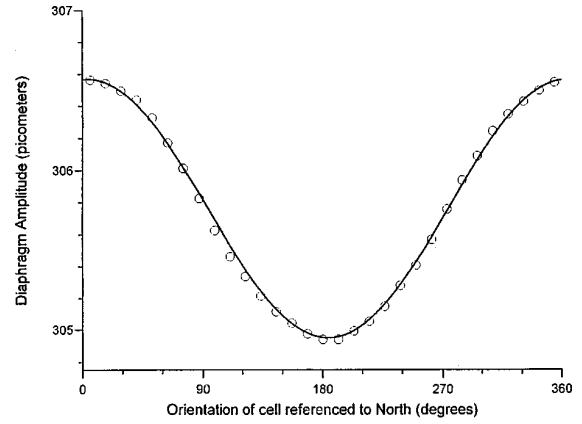


FIG. 14. The critical oscillation amplitude of the diaphragm as a function of orientation of the torus plane. The normal to the torus plane points northward at 0 deg.

the stochastic width of the phase slip critical velocity, f_o is the frequency of the diaphragm-aperture oscillator, and τ is the measurement time. It remains to be seen whether future development will attain the full theoretical limit of sensitivity for multiturn, large-diameter superfluid gyroscopes.

Sensitive rotation detectors are important to several areas of science, including general relativity and geodesy. Perhaps the future will show that the interesting physics which has emerged from the JA equation will lead to unexpected new technology.

IV. SUMMARY AND RECENT DEVELOPMENTS

This article has reviewed some examples of the use of the Josephson-Anderson phase evolution equation. We have tried to show that the equation provides an elegant short cut to certain predictions (such as the frequency of the precessing vortex and the size of a phase slip) that involve the complex motion of quantized vortices. These same predictions by other methods require a detailed knowledge of vortex motion and involve considerable computational effort. The experiments that illustrate this point have led to an enhanced understanding of vortex phenomena, including the vortex helicopter and the nucleation of vortices. It is satisfying that out of this somewhat esoteric exercise a new technology of inertial sensors may evolve.

Very recently the JA equation has found a new and important role in the realm of superfluid physics. We have discovered (Pereversev *et al.*, 1997) that an array of several thousand submicrometer-sized apertures behaves as a single coherent weak link between two reservoirs of superfluid ^3He . In the experimental arrangement one can simultaneously determine the mass current $I(t)$ through the weak links and the pressure head $\Delta P(t)$ across them. We desired to determine the relation between the current and the corresponding phase difference $\phi(t)$. This was accomplished by integrating the JA equation:

$$\Delta\phi(t) = -\frac{2m_3}{\rho\hbar} \int_0^t \Delta P(t) dt. \quad (19)$$

Thus knowledge of the time evolution of the pressure head yields the time dependence of $\phi(t)$. Combining this function with the measured current generates the current phase relation $I(\phi)$. The experiment showed that the weak-link array behaves like an ideal Josephson junction at high temperatures, i.e., $I(\phi)$ is sinusoidal (Backhaus *et al.*, 1997). At lower temperatures the function continuously evolved toward that of an ordinary tube connection.

The integral form of the JA equation provides an important measure of the quantum phase difference and will undoubtedly play a significant role in future experiments with ^3He weak links.

ACKNOWLEDGMENTS

The results described here were obtained through the author's enjoyable collaboration with a group of dedicated graduate students and postdoctoral visitors. I wish to acknowledge efforts by A. Amar, S. Backhaus, N. Bruckner, J. Close, Yu. Mukharsky, Y. Sasaki, K. Schwab, J. Steinhauer, and R. Zieve. K. Schwab generated Fig. 1. J. C. Davis was a close collaborator through much of the work described. Conversations with O. Avenel, E. Varoquaux, S. Vitale, and W. Zimmermann, Jr., have been very helpful in understanding the physics of ^4He phase slips. The work was supported over the past several years by grants from the National Science Foundation and the Office of Naval Research.

REFERENCES

- Allen, J. F., and A. D. Misener, 1939, Proc. R. Soc. London, Ser. A **172**, 467.
- Amar, A., R. L. Lozes, and R. E. Packard, 1993, J. Vac. Sci. Technol. B **11**, 259.
- Amar, A., Y. Sasaki, R. Lozes, J. C. Davis, and R. E. Packard, 1992, Phys. Rev. Lett. **68**, 2624.
- Anderson, P. W., 1966, Rev. Mod. Phys. **38**, 298.
- Avenel, O., R. Aarts, G. G. Ihas, and E. Varoquaux, 1994, in *Proceedings of the 20th International Conference on Low Temperature Physics*, Physica B **194–196**, 491.
- Avenel, O., P. Hakonen, and E. Varoquaux, 1997, Phys. Rev. Lett. **78**, 3602.
- Avenel, O., G. G. Ihas, and E. Varoquaux, 1993, J. Low Temp. Phys. **93**, 1031.
- Avenel, O., and E. Varoquaux, 1987, in *18th International Conference on Low Temperature Physics*, Jpn. J. Appl. Phys. Suppl. **26**, 1798.
- Backhaus, S., S. V. Pereversev, A. Loshak, J. C. Davis, and R. E. Packard, 1997, Science **278**, 1435.
- Burkhart, S., M. Bernard, O. Avenel, and E. Varoquaux, 1994, Phys. Rev. Lett. **72**, 380.
- Close, J., R. Zieve, J. C. Davis, and R. E. Packard, 1990, Physica B **165 & 166**, 57.
- Davis, J. C., R. J. Zieve, J. D. Close, and R. E. Packard, 1990, Phys. Rev. Lett. **66**, 329.
- Donnelly, R. G., 1991, *Quantized Vortices in Helium II* (Cambridge University Press, New York).
- Feynman, R. P., 1955, in *Progress in Low Temperature Physics*, edited by C. J. Gorter (North-Holland, Amsterdam), p. 17.
- Guénault, A. M., V. Keith, C. J. Kennedy, S. G. Mussett, and G. R. Pickett, 1986, J. Low Temp. Phys. **62**, 511.
- Hall, H. E., and W. F. Vinen, 1956, Proc. R. Soc. London, Ser. A **238**, 204, 215.
- Huggins, E. R., 1970, Phys. Rev. A **1**, 327 and 332.
- Josephson, B. D., 1962, Phys. Lett. **1**, 251.
- Kapitza, P., 1938, Nature (London) **141**, 74.
- Krusius, M., 1993, J. Low Temp. Phys. **91**, 233.
- Landau, L. D., 1941, J. Phys. (Moscow) **5**, 71.
- Lindensmith, C. A., 1996, Ph.D. thesis (University of Minnesota).
- Lindensmith, C. A., J. A. Flaten, and W. Zimmermann, 1996, in *Proceedings of the 21st International Conference on Low Temperature Physics*, Czech. J. Phys. **46**, 131.
- London, F., 1954, *Superfluids Vol. II, Macroscopic Theory of Superfluid Helium* (Dover, New York).
- Misirpashaev, T. Sh., and G. E. Volovik, 1992, Pis'ma Zh. Eksp. Teor. Fiz. **56**, 40 [JETP Lett. **56**, 41 (1992)].
- Morrison, H. L., and J. V. Lindsey, 1977, J. Low Temp. Phys. **26**, 899.
- Onsager, L., 1949, Nuovo Cimento **6** suppl. 2, 249.
- Packard, R. E., and S. Vitale, 1992, Phys. Rev. B **46**, 3540.
- Paik, H. J., 1976, J. Appl. Phys. **47**, 1168.
- Pereversev, S. V., A. Loshak, S. Backhaus, J. C. Davis, and R. E. Packard, 1997, Nature (London) **388**, 449.
- Rayfield, G. W., and F. Reif, 1964, Phys. Rev. **136**, 1194.
- Schwab, K., 1996, Ph.D. thesis (University of California-Berkeley).
- Schwab, K., N. Bruckner, and R. E. Packard, 1997, Nature (London) **368**, 585.
- Schwarz, K., 1990, Phys. Rev. Lett. **64**, 1130.
- Schwarz, K. W., 1993a, Phys. Rev. B **47**, 12030.
- Schwarz, K. W., 1993b, Phys. Rev. Lett. **71**, 259.
- Shiflett, G. M., and G. B. Hess, 1995, J. Low Temp. Phys. **98**, 591.
- Sonin, E. B., 1994, J. Low Temp. Phys. **97**, 145.
- Steinhauer, J., K. Schwab, Yu. Mukharsky, J. C. Davis, and R. E. Packard, 1995a, Phys. Rev. Lett. **74**, 5056.
- Steinhauer, J., K. Schwab, Yu. Mukharsky, J. C. Davis, and R. E. Packard, 1995b, J. Low Temp. Phys. **100**, 281.
- Tisza, L., 1938, Nature (London) **141**, 913.
- Varoquaux, E., W. Zimmermann, Jr., and O. Avenel, 1991, in *Excitation in Two-Dimensional and Three-Dimensional Quantum Fluids*, edited by A. F. G. Wyatt and H. J. Lauter (Plenum, New York), p. 343.
- Vinen, W. F., 1961, Proc. R. Soc. London, Ser. A **260**, 218.
- Whitmore, S. C., and W. Zimmermann Jr., 1968, Phys. Rev. **166**, 181.
- Yarmchuk, E. J., M. J. V. Gordon, and R. E. Packard, 1979, Phys. Rev. Lett. **43**, 214.
- Zieve, R. J., 1992, Ph.D. thesis (University of California-Berkeley).
- Zieve, R. J., J. D. Close, J. C. Davis, and R. E. Packard, 1993, J. Low Temp. Phys. **90**, 243.
- Zieve, R. J., Yu. Mukharsky, J. D. Close, J. C. Davis, and R. E. Packard, 1992, Phys. Rev. Lett. **68**, 1327.
- Zimmermann, W. Jr., 1993, J. Low Temp. Phys. **93**, 1003.
- Zimmermann, W. Jr., 1996, Contemp. Phys. **37**, 219.